

Raman-active phonons and their doping dependence in Pb-based cuprate superconductors

Masato Kakihana,* Minoru Osada,[†] and Atsuyoshi Inoue

Materials and Structures Laboratory, Tokyo Institute of Technology, Nagatsuta 4259, Midori-ku, Yokohama 226-8503, Japan

Takashi Noji, Masatsune Kato, and Yoji Koike

Department of Applied Physics, Graduate School of Engineering, Tohoku University, Aoba-yama 08, Aoba-ku, Sendai 980-8579, Japan

Mikael Käll and Lars Börjesson

Department of Applied Physics, Chalmers University of Technology, S412-96, Göteborg, Sweden

(Received 12 March 1999)

The phonon Raman spectra of $(\text{Pb}_2\text{Cu})\text{Sr}_2\text{Y}_{1-x}\text{Ca}_x\text{Cu}_2\text{O}_{8+d}$ (Pb3212), $(\text{Pb}_2\text{Cu})\text{Sr}_{0.9}\text{La}_{1.1}\text{CuO}_{6+d}$ (Pb3201), and $(\text{Pb}_{0.5}\text{Cu}_{0.5})\text{Sr}_2\text{YCu}_2\text{O}_{7+d}$ (Pd1212) are investigated and phonon assignments compatible with the layer stacking sequences found in these Pb-based cuprate superconductors are proposed. In particular, the assignment of the 480- and 570- cm^{-1} phonons to oxygen in the PbO and SrO layers, respectively, is established. In the case of Pb3212 we find that the intensities of the CuO_2 -plane phonons decrease with increasing carrier concentration. This effect appears to be, at least partly, due to an interaction between the CuO_2 -plane phonons and Raman scattering associated with conduction carriers. [S0163-1829(99)02133-5]

Inelastic light-scattering experiments on high- T_c superconductors has yielded a wealth of fundamental information on the superconducting gap, magnetic excitations, band structure, and electron-phonon coupling. As the Raman spectrum of a cuprate is usually dominated by phonons, a thorough understanding of the frequencies and eigenvectors of the Raman-active vibrational modes, as well as their dependence on doping and structure, becomes important.

In this brief report we reinvestigate the Raman phonon spectrum of one of the less common cuprates: $(\text{Pb}_2\text{Cu})\text{Sr}_2\text{LCu}_2\text{O}_{8+d}$ (Pb3212), where L represents a lanthanide, e.g., Y. The Pb3212 cuprates were shown to be high- T_c superconductors, with a highest T_c near 80 K, by Cava *et al.*¹ The appearance of superconductivity has been linked to a transfer of holes from the Ca dopant ions to the conducting CuO_2 planes,^{2,3} in a way similar to what has been observed in $\text{YBa}_2\text{Cu}_3\text{O}_{6+d}$ (Y123) with increasing oxygen content (d).^{4,5}

Only a limited number of Raman-scattering studies on Pb3212 have been reported (Refs. 6–10) and the assignments of phonon eigenmodes is not entirely clear. The two high-frequency oxygen modes, at 480 and 570 cm^{-1} respectively, have proved particularly troublesome. We have previously been able to resolve a similar controversy in the family of Bi-based cuprates^{11–13} by comparing structures with different stacking sequence. There it was found that the two analogous oxygen modes, which occurs at 460 and 630 cm^{-1} in the Bi-based cuprates, were due to the motion of oxygen in the BiO layers and the SrO layers, respectively. These assignments have recently received further support from isotopic exchange experiments.¹⁴ Here we compare the Raman phonon spectrum of Pb3212, $(\text{Pb}_2\text{Cu})\text{Sr}_{0.9}\text{La}_{1.1}\text{CuO}_{6+d}$ (Pb3201), and $(\text{Pb}_{1-x}\text{Cu}_x)\text{Sr}_2\text{LCu}_2\text{O}_{7+d}$ (Pd1212) and reach a similar conclusion. We also investigate how the aliovalent substitution of Ca^{2+} for Y^{3+} influences the phonon Raman spectrum of Pb3212. In our previous report on $\text{Bi}_2\text{Sr}_2\text{Y}_{1-x}\text{Ca}_x\text{Cu}_2\text{O}_{8+d}$,¹¹ we found that the increase in the CuO_2 -plane carrier concentration, which occurs upon Ca doping, is directly reflected in an intensity decrease of pho-

non modes involving the CuO_2 planes. We find a very similar effect in the Pb3212 system and discuss its possible physical origin.

Samples of polycrystalline $(\text{Pb}_2\text{Cu})\text{Sr}_2\text{Y}_{1-x}\text{Ca}_x\text{Cu}_2\text{O}_{8+d}$ ($x=0-0.5$), $(\text{Pb}_2\text{Cu})\text{Sr}_{0.9}\text{La}_{1.1}\text{CuO}_{6+d}$, and $(\text{Pb}_{0.5}\text{Cu}_{0.5})\text{Sr}_2\text{YCu}_2\text{O}_{7+d}$ were prepared by solid-state reaction or polymerized complex techniques, as described in detail in Refs. 3, 15, and 16, respectively. For comparison a single crystal of $(\text{Pb}_2\text{Cu})\text{Sr}_2\text{Y}_{0.5}\text{Ca}_{0.5}\text{Cu}_2\text{O}_{8+d}$ ($T_c=75$ K), grown by the PbO-NaCl flux method,¹⁷ was investigated. All samples used for Raman measurements were of single phase as confirmed by x-ray diffraction.^{3,15,16} Room-temperature Raman spectra were excited with 514.5 nm line of an Ar laser (~ 1 mW incident power) and the scattered light was analyzed with a triple spectrometer (Jobin Yvon/Atago Busan R-64000) equipped with a liquid-nitrogen-cooled CCD detector. The spatial resolution (laser spot-size) was ~ 3 μm whereas the spectral resolution was 3–4 cm^{-1} .

The crystal structures of the Pb-based cuprates are pseudotetragonal, with a weak orthorhombic distortion probably originating in the PbO planes.¹⁸ In the ideal tetragonal approximation, where the unit cell contains one formula unit, the stacking sequences of the different layers along the c axis can be written as

$$-\text{CuO}_2-\text{SrO}-\text{PbO}-\text{Cu}-\text{PbO}-\text{SrO}-\text{CuO}_2-\text{Pb3201}$$

$$-\text{Y}-\text{CuO}_2-\text{SrO}-\text{PbO}-\text{Cu}-\text{PbO}-\text{SrO}-\text{CuO}_2-\text{Y}-$$

Pb3212

$$-\text{Y}-\text{CuO}_2-\text{SrO}-\text{PbO}-\text{SrO}-\text{CuO}_2-\text{Y}-\text{Pb1212}$$

Here the vertical bars mark the repetition unit and layers written in bold face have *inversion symmetry*, and do therefore not contribute to any Raman-active modes. In Pb3212 and Pb1212 we thus expect three independent c -axis vibrations associated with CuO_2 plane (i.e., one in-phase $\text{O}_{\text{Cu}} A_{1g}$, one out-of-phase $\text{O}_{\text{Cu}} B_{1g}$ and one metallic Cu A_{1g}

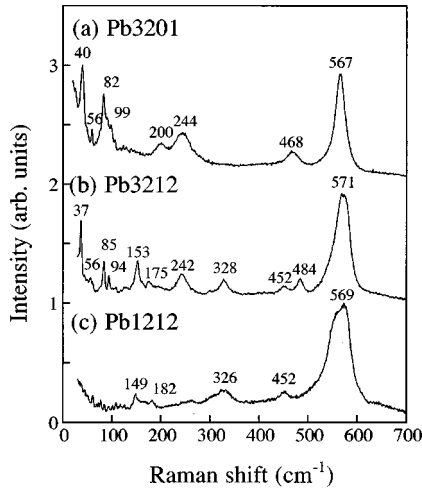


FIG. 1. Unpolarized micro-Raman spectra of $(\text{Pb}_2\text{Cu})\text{Sr}_{0.9}\text{La}_{1.1}\text{CuO}_{6.21}$ (a), $(\text{Pb}_2\text{Cu})\text{Sr}_2\text{YCu}_2\text{O}_{8.23}$ (b), and $(\text{Pb}_{0.5}\text{Cu}_{0.5})\text{Sr}_2\text{YCu}_2\text{O}_{7.20}$ (c) polycrystalline samples at room temperature. Pure rotational Raman lines of N_2 and O_2 in ambient air sometimes interfere with the observation of Raman scattering from samples below 150 cm^{-1} . However, since the position of these rotational lines are precisely known, they can be discriminated from the Raman lines from samples. The bands observed at 40, 56, 82, and 99 cm^{-1} for Pb3201 and at 37, 56, 85, 94, and 153 cm^{-1} are originated from samples.

mode), that should not be observed in Pb3201. Similarly, two SrO c -axis vibrations should be visible in all three compounds while the PbO planes should contribute to two Raman-active c -axis modes in both Pb3201 and Pb3212 but not in Pb1212. The same arguments also apply for vibrations along the a and b axis, but previous investigations of high- T_c cuprates shows that these modes are usually too weak to be detected in measurements on polycrystalline samples.

In Fig. 1 we show unpolarized Raman spectra of the three Pb-based compounds. A comparison of the spectra, with the simple rules outlined above in mind, indicate that the peaks at around 150, 328, and 452 cm^{-1} originate in the CuO_2 planes while the intense peak at $\sim 570\text{ cm}^{-1}$ and the weak mode at $175\text{--}200\text{ cm}^{-1}$ belong to the SrO layers. Peaks common to Pb3201 and Pb3212 but absent in the Pb1212 spectrum, i.e., PbO vibrations, can be found at around 40, 56, 85, 94, 242, and $468/484\text{ cm}^{-1}$. Assuming that the vibrational frequencies are roughly inversely proportional to the square root of the ionic mass we propose the assignments summarized in Table I.

Table I also includes phonon symmetries for those layers where the number of modes coincides with that expected for a tetragonal unit cell. The B_{1g} character of the 326 cm^{-1} mode has been observed in several previous reports,¹¹ and is also evident in the single-crystal spectra shown in Fig. 2. One may also notice the strongly zz polarized character of the 571 cm^{-1} phonon in Fig. 2, a feature shared with the analogous apical-oxygen phonon in the Bi-based cuprates.^{11–13} It is also clear from Table I that the tetragonal approximation fails for the PbO layers, since six PbO-related modes are observed experimentally, while only two modes are expected for a tetragonal unit cell. The number of low-frequency Pb modes suggests that a proper unit cell should actually include four distinct Pb sites. The origin of the broad

TABLE I. Frequencies (in cm^{-1}) and proposed assignments for the Raman-active c -axis vibrations in $(\text{Pb}_2\text{Cu})\text{Sr}_{0.9}\text{La}_{1.1}\text{CuO}_{6.21}$ (Pb3201), $(\text{Pb}_2\text{Cu})\text{Sr}_2\text{YCu}_2\text{O}_{8.23}$ (Pb3212), and $(\text{Pb}_{0.5}\text{Cu}_{0.5})\text{Sr}_2\text{YCu}_2\text{O}_{7.20}$ (Pb1212).

Layer	Ion/symmetry	Pb3201	Pb3212	Pb1212
CuO_2	Cu/A_{1g}	a	153	149
CuO_2	$\text{O}_{\text{Cu}}/A_{1g}$	a	452	452
CuO_2	$\text{O}_{\text{Cu}}/B_{1g}$	a	326	328
SrO	Sr/A_{1g}	200	175	182
SrO	$\text{O}_{\text{Sr}}/A_{1g}$	567	571	569
PbO	Pb/A_{1g}	40/56/82/99	37/56/85/94	a
PbO	$[\text{O}_{\text{Pb}}]^c$	$[244]^c$	$[242]^c$	a
PbO	$\text{O}_{\text{Pb}}/A_{1g}$	468	484	a
Group-theoretical analysis ^b		$4A_{1g}$	$6A_{1g}+1B_{1g}$	$4A_{1g}+1B_{1g}$

^aRaman forbidden (where layers are at an *inversion center*).

^bA first approximation in the ideal tetragonal unit cell.

^cA mode associated with weakly bound interstitial oxygens within PbO layers.

244 cm^{-1} phonon is unclear, one possibility is a mode associated with weakly bound interstitial oxygens. The highest frequency PbO-related mode can safely be assigned to the oxygen-stretching vibration, which would have had A_{1g} character in the tetragonal unit cell.

The assignments proposed for Pb3212 in Table I are similar to those of Cardona and co-workers given in Refs. 6–8. However, this group later reversed the assignments of the two high-frequency oxygen modes (Refs. 9 and 19) based on the lattice-dynamical calculations of Kress *et al.*²⁰ From the comparison of different Pb-based compounds presented above it should now be clear that the 484- and 571 cm^{-1} phonons in Pb3212 are oxygen-stretching modes originating in the PbO and SrO layers, respectively.

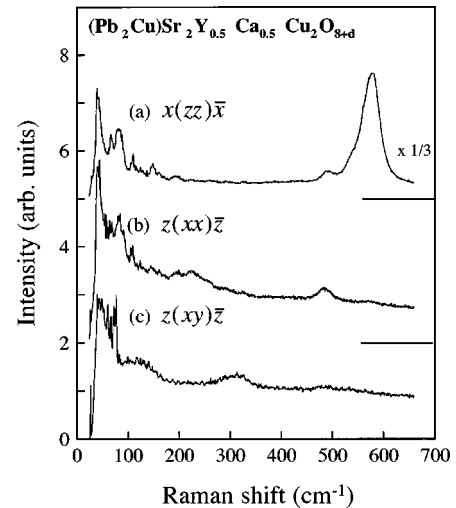


FIG. 2. Polarized micro-Raman spectra of a $(\text{Pb}_2\text{Cu})\text{Sr}_2\text{Y}_{0.5}\text{Ca}_{0.5}\text{Cu}_2\text{O}_{8+d}$ single crystal at room temperature in scattering configurations (a) $x(\overline{z}z)x$, (b) $z(xx)\overline{z}$, and (c) $z(xy)\overline{z}$. The short lines denote the zero-intensity level for the spectrum immediately above. The scattering factors are also shown. Some of the lines below 150 cm^{-1} , most notably in (b) and (c) are due to rotational lines of air.

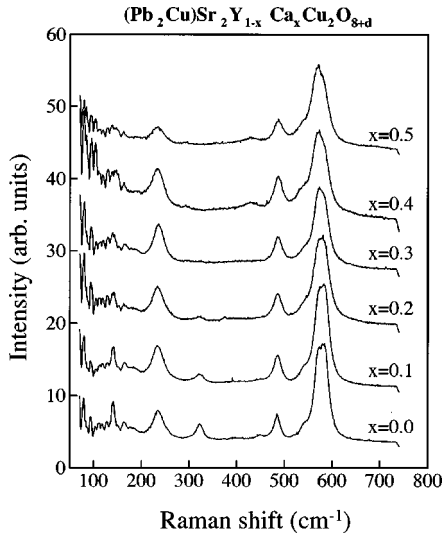


FIG. 3. Unpolarized micro-Raman spectra of $(\text{Pb}_2\text{Cu})\text{Sr}_2\text{Y}_{1-x}\text{Ca}_x\text{Cu}_2\text{O}_{8+d}$ polycrystalline samples for different Ca contents at room temperature. Some of the lines below 150 cm^{-1} are due to rotational lines of air.

We now turn to the variation in phonon spectra with doping. Figure 3 shows unpolarized Raman measurements of polycrystalline $(\text{Pb}_2\text{Cu})\text{Sr}_2\text{Y}_{1-x}\text{Ca}_x\text{Cu}_2\text{O}_{8+d}$ samples for different degrees of Ca doping. We find that the two vibrational modes involving atoms in the CuO_2 planes, i.e., B_{1g} O_{Cu} at 326 cm^{-1} and A_{1g} Cu at 151 cm^{-1} decrease in intensity relative to the non- CuO_2 -related phonons for increasing Ca content. Similar intensity decreases have been observed for the corresponding CuO_2 -plane modes in $\text{Bi}_2\text{Sr}_2\text{Y}_{1-x}\text{Ca}_x\text{Cu}_2\text{O}_{8+d}$ (Ref. 11) and $\text{Y}_{1-x}\text{Ca}_x\text{Ba}_2\text{Cu}_3\text{O}_{6+d}$ (Refs. 21–24) when the carrier concentration is increased through Ca substitution and oxygen doping, respectively. The fact that the effect is qualitatively similar for modes of different symmetry and for different cuprate structures indicates that the origin is not simply a shift in some specific electronic resonance or a result of a difference in O-Y and O-Ca bond polarizabilities, as suggested by Liu *et al.*⁷ One may also note that a variation in the macroscopic optical properties (i.e., optical penetration depth and refractive index) with carrier concentration changes the overall Raman scattering intensity, whereas Fig. 3 shows a change in relative phonon intensities.

In Fig. 4 we show micro-Raman spectra of the B_{1g} phonon, measured in the xy -polarization configuration, while Fig. 5 shows a comparison between the integrated phonon intensity and the corresponding critical temperatures T_c for $0 \leq x \leq 0.5$.³ It is interesting that both the B_{1g} O_{Cu} intensity and T_c show the same abrupt jump between $x=0.1$ and 0.2 , and that they both tend to level off to a given value for higher x . This correlation clearly signals a close relationship between the phonon and electronic properties of the CuO_2 planes. A clue to the nature of this relationship can be found in Fig. 4. Here it is seen that the intensity decrease of the B_{1g} O_{Cu} phonon is accompanied by a change in line shape when the Ca content increases from $x=0$ up to $x=0.2$. For the $x=0.2$ sample in particular, the phonon line exhibits a highly asymmetric shape which is well described by the Fano function:

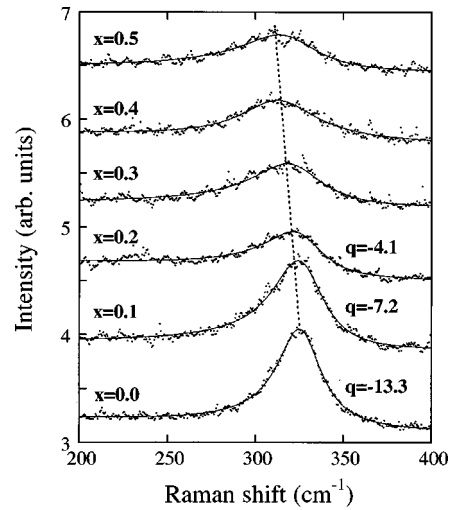


FIG. 4. Depolarized micro-Raman spectra (approximate xy -polarization configuration) of $(\text{Pb}_2\text{Cu})\text{Sr}_2\text{Y}_{1-x}\text{Ca}_x\text{Cu}_2\text{O}_{8+d}$ crystal-lites at room temperature. The spectra show the B_{1g} CuO_2 -plane phonon for increasing Ca content x together with fits to the Fano line shape (see text). The variation in phonon frequency with x is indicated by the dashed line.

$$I(\omega) \sim [q + (\omega - \omega_p)/\Gamma]^2 / [1 + (\omega - \omega_p)^2/\Gamma^2],$$

where ω_p and Γ are the phonon frequency and linewidth (half width at half maximum), respectively, and q is inversely proportional to the phonon asymmetry.¹⁹ In the cuprates, the physical origin of the line-shape asymmetry is thought to be a coherent modulation of electronic Raman scattering, evident as a uniform continuum in Fig. 4, by the phonon. Microscopic descriptions based on phonon-modulated interband excitations has been given by, e.g., Monien and Zavadovski²⁵ and, recently, by Devereaux *et al.*²⁶ However, for a qualitative picture the simple approach outlined in Ref. 19 suffices. The asymmetry, measured as $1/q$, is in a first approximation proportional to $V \cdot I_e$, where V measures the coupling between the electronic and phonon degrees of freedom and I_e is the intensity of that part of the electronic background which interacts with the phonon. The integrated intensity of the Fano line shape is

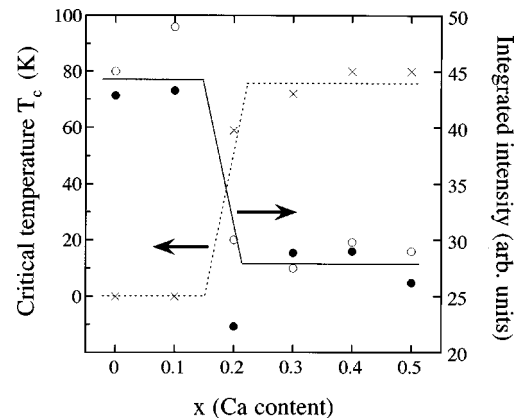


FIG. 5. The integrated intensity of the B_{1g} CuO_2 -plane phonon and the critical temperature T_c versus Ca content x (T_c data extracted from Ref. 3). Open and solid symbols show the phonon intensity as estimated by Lorentzian and Fano curve fits to the data displayed in Fig. 4, respectively.

simply $I = I_p(1 - 1/q^2)$, where I_p is the “bare” phonon intensity. Under the assumption that I_p and V are more-or-less constant, the increasing asymmetry and the decreasing integrated intensity thus both indicate an increase in I_e induced by Ca substitution.

For $x = 0.3$ the phonon asymmetry is no longer as evident as for the $x = 0.2$ sample and the line shape is, in fact, well described by a symmetric Lorentzian function. The integrated intensity is, however, still markedly lower than for the $0 < x < 0.1$ samples. We interpret this reversion to a symmetric shape as an effect of substitutional disorder. It is well known that the B_{1g} O_{Cu} phonon frequency is highly dependent on the size of the ion separating the two CuO_2 planes.^{6,19} As Ca^{2+} ($r \approx 0.99$ Å) is much larger than Y^{3+} ($r \approx 0.89$ Å), we thus expect an additional phonon broadening, which would tend to hide the electronically induced asymmetry, for intermediate compositions as well as a phonon softening due to the lattice expansion induced by Ca substitution. Both the softening and the broadening effects can be seen in Fig. 4 when comparing, e.g., the $x = 0$ and the $x = 0.5$ spectra.

Based on the discussion above we suggest that the decrease of phonon intensity with doping is partly due to an increase in electronic Raman scattering. Although this effect may even be dominant in the case of the B_{1g} O_{Cu} phonon,

one should note that the symmetric Cu phonon exhibits a similar intensity variation despite a negligible coupling to the electronic background. This suggests that additional effects are important and indicate the need for further experimental and theoretical investigations.

In summary, we have investigated phonon Raman spectra of $(Pb_2Cu)Sr_2Y_{1-x}Ca_xCu_2O_{8+d}$, $(Pb_2Cu)Sr_{0.9}La_{1.1}CuO_{6+d}$, and $(Pb_{0.5}Cu_{0.5})Sr_2YCu_2O_{7+d}$. By comparing structures with the different layer stacking we proposed phonon assignments compatible with these Pb-based cuprates. In particular, the assignment of the 480 and 570 cm^{-1} phonons to oxygen in the PbO and SrO layers, respectively, is established. In the case of $(Pb_2Cu)Sr_2Y_{1-x}Ca_xCu_2O_{8+d}$, we found that the intensity of the CuO_2 -plane phonons decreases with increasing carrier concentration, and the B_{1g} O_{Cu} intensity versus x curve correlates to the dependence of T_c versus x . We argue that this effect is due to an interaction between the CuO_2 -plane phonons and Raman scattering associated with conduction carriers.

We gratefully acknowledge Dr. A. Bock (Universität Hamburg) for many stimulating discussions on the Fano effect. We thank Professor M. Yashima and Professor M. Yoshimura (Tokyo Institute of Technology) for their encouragement throughout this work.

*Author to whom correspondence should be addressed. Electronic address: kakihana@rlem.titech.ac.jp

[†]Present address: The Institute of Physical and Chemical Research (RIKEN), Hirosawa 2-1, Wako, Saitama 351-0198, Japan.

¹R. J. Cava, B. Batlogg, J. J. Krajewski, L. W. Rupp, L. F. Schneemeyer, T. Siegrist, R. B. van Dover, P. Marsh, W. F. Peck, Jr., P. K. Gallagher, S. H. Glarum, J. H. Marshall, R. C. Farrow, J. V. Waszczak, R. Hull, and P. Trevor, *Nature (London)* **336**, 211 (1988).

²J. E. Jorgensen and N. H. Andersen, *Physica C* **218**, 43 (1993).

³Y. Koike, M. Masuzawa, T. Noji, H. Sunagawa, H. Kawabe, N. Kobayashi, and Y. Saito, *Physica C* **170**, 130 (1990).

⁴R. J. Cava, A. W. Hewat, E. A. Hewat, B. Batlogg, M. Marezio, K. M. Rabe, J. J. Krajewski, W. F. Peck, Jr., and L. W. Rupp, Jr., *Physica C* **165**, 419 (1990).

⁵J. D. Jorgensen, B. W. Veal, A. P. Paulikas, L. J. Nowicki, G. W. Crabtree, H. Claus, and W. K. Kwok, *Phys. Rev. B* **41**, 1863 (1990).

⁶C. Thomsen, M. Cardona, R. Liu, H. Mattausch, W. König, F. Garcia-Alvarado, B. Suarez, E. Moran, and M. Alario-Franco, *Solid State Commun.* **69**, 857 (1989).

⁷R. Liu, M. Cardona, B. Gegenheimer, E. T. Heyen, and C. Thomsen, *Phys. Rev. B* **40**, 2654 (1989).

⁸E. T. Heyen, R. Liu, M. Garriga, B. Gegenheimer, C. Thomsen, and M. Cardona, *Phys. Rev. B* **41**, 830 (1990).

⁹R. Wegerer, C. Thomsen, T. Ruf, E. Schönherr, M. Cardona, M. Reedyk, J. S. Xue, J. E. Greedan, and A. Furrer, *Phys. Rev. B* **48**, 6413 (1993).

¹⁰S. Sugai, N. Kitamori, N. Yamane, T. Noji, and Y. Koike, *Physica C* **263**, 363 (1996).

¹¹M. Kakihana, M. Osada, M. Käll, L. Börjesson, H. Mazaki, H. Yasuoka, M. Yashima, and M. Yoshimura, *Phys. Rev. B* **53**, 11 796 (1996).

¹²M. Osada, M. Kakihana, M. Käll, L. Börjesson, A. Inoue, and M. Yashima, *Phys. Rev. B* **56**, 2847 (1997).

¹³M. Osada, M. Kakihana, M. Käll, and L. Börjesson, *J. Phys. Chem. Solids* **59**, 2003 (1998).

¹⁴A. E. Pantoja, D. M. Pooke, H. J. Trodahl, and J. C. Irwin, *Phys. Rev. B* **58**, 5219 (1998).

¹⁵M. Kakihana, *J. Sol-Gel Sci. Technol.* **6**, 7 (1996).

¹⁶M. Kato, T. Miyajima, A. Sakuma, T. Noji, Y. Koike, A. Fujiwara, and Y. Saito, *Physica C* **244**, 263 (1995).

¹⁷T. Noji, Y. Koike, K. Ohtsubo, S. Shiga, M. Kato, A. Fujiwara, and Y. Saito, *Jpn. J. Appl. Phys., Part 1* **33**, 2515 (1994).

¹⁸R. J. Cava, M. Marezio, J. J. Krajewski, W. F. Peck, Jr., A. Santoro, and F. Beck, *Physica C* **157**, 272 (1989).

¹⁹See, e.g., C. Thomsen, in *Light Scattering in Solids VI*, edited by M. Cardona and G. Güntherodt (Springer-Verlag, Berlin, 1991), Chap. 6.

²⁰W. Kress, J. Prade, U. Schröder, A. D. Kulkarni, and F. W. de Wette, *Physica C* **162-164**, 1345 (1989).

²¹M. Hangyo, S. Nakashima, K. Mizoguchi, A. Fujii, A. Mitsuishi, and T. Yotsuya, *Solid State Commun.* **65**, 835 (1988).

²²R. Liu, C. Thomsen, W. Kress, M. Cardona, B. Gegenheimer, F. W. de Wette, J. Prade, A. D. Kulkarni, and U. Schröder, *Phys. Rev. B* **37**, 7971 (1988).

²³C. Thomsen, R. Liu, M. Bauer, A. Wittlin, L. Genzel, M. Cardona, E. Schönherr, W. Bauhofer, and W. König, *Solid State Commun.* **65**, 55 (1988).

²⁴P. Berastegui, S. G. Eriksson, L. G. Johansson, M. Kakihana, M. Osada, H. Mazaki, and S. Tochihara, *J. Solid State Chem.* **127**, 56 (1996).

²⁵H. Monien and A. Zawadowski, *Phys. Rev. Lett.* **63**, 911 (1989).

²⁶T. P. Devereaux, A. Virostek, and A. Zawadowski, *Phys. Rev. B* **51**, 505 (1995).